SELECTION AND MEASUREMENT OF RF PHASE WIDTH
OF THE K1200 CYCLOTRON BEAM

J. Bailey, J. Kuchar, F. Marti, and J. Yurkon*
NSCL, MSU, East Lansing, MI, 48824, USA

and

J. Nolen
Physics Division, Argonne National Lab., Argonne, IL, 60439,USA

and

D. Rifuggiatto
INFN, Catania, Italy

ABSTRACT

Reductions to 4° FWHM in RF phase width of the K1200 extracted beam have been achieved with the use of internal radial slits. Beam losses using the phase slits have been minimized to 70%. Rapid measurements of the time structure of the extracted beam have been obtained using a silicon detector placed in the beam shortly after extraction, with attenuators in the injection beam line. An internal timing probe using a silicon detector has been designed, and is under construction.
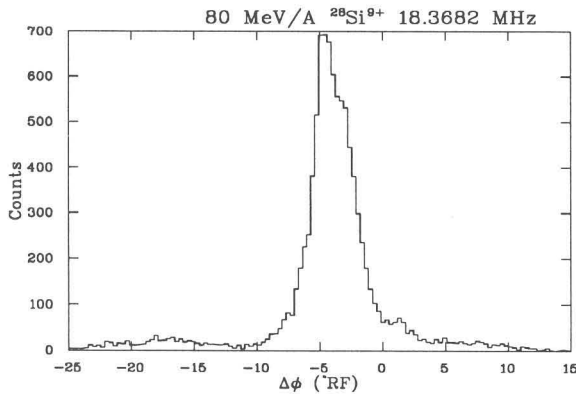
Figure 1. The best extracted beam phase width to date. The FWHM is 3.6° RF, or .55 ns at this frequency. Lower widths in the main peak have been achieved, but with larger shoulders and satellites.

1. INTRODUCTION

The RF phase acceptance determined by the central region of the K1200 cyclotron is 40° RF.[1,2] The use of a buncher to further restrict the RF phase at injection, with just first, or both first and second harmonics, is limited by debunching in time during traversal of the yoke and spiral inflector.[2] The first harmonic buncher calculations show enhancement over the entire acceptance range with a preferential enhancement of a

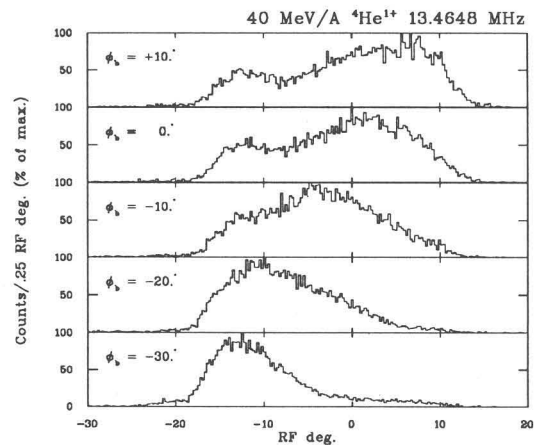**Figure 2.** Measured time structure of the beam after extraction for buncher phase $\phi_b = -30°$ to $+10°$. Note the broad base even when the buncher is well tuned. Also, all phases measured to date have been relative, the zeros are not absolute.

narrower range. Multi-turn extraction adds further complications, but Fig. 2. shows that this effect can be seen after extraction.

2. PHASE SLIT DESIGN

Further reductions in transmission of RF phase can be obtained with internal cuts. Holes through the yoke, hill, and liner at 7 in. radius permit access to a region of the cyclotron where the turns are separated, and the beam energy is low, $\sim 1/40$th of the energy at extraction. At this radius correlations between RF phase and radius can exist due to differences in centering errors, and/or a phase dependent difference in energy, which to first order is $\Delta E(\phi) = -\Delta\phi \int \sin(\phi) dE$.[3]

2.1. Mechanical Design

The slits are a modified version of those used by B. Milton in the K500 cyclotron.[3,4] They are tungsten pins with a diameter of 0.094 in. Since $\nu_r \simeq 1$, the particles rotate in (r, p_r) phase space approximately once per
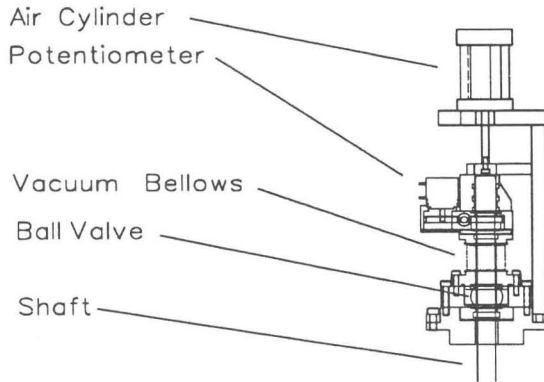
Figure 3. Part of the Phase Slit Drive. Shown are the shaft, potentiometer, air cylinder and vacuum bellows for insertion, and ball valve used to maintain vacuum when changing tips.

complete revolution in the machine. Thus a pin placed between turns will make radial cuts similar to those of radial slits about the second turn being cut. Slits separated by 120°, make cuts in (r, p_r) phase space that are rotated by $\sim 120°$ (see Fig. 4.), if, between the slits, there are zero or two orbit crossovers, of the central phase being transmitted and the phase being cut. Each orbit crossover inverts the $r - \phi$ correlation, switching the side of the pin that makes the cut. Thus the cut makes an additional 180° rotation in (r, p_r) phase space per orbit crossover. We are currently using two slits 120° apart.

Other features include remotely controlled insertion, retraction, and rotation (see Fig. 3.) The pin is mounted slightly off-center, so rotating it adjusts its radius. Electric motors mounted 8 ft. above the cap, protected with 1/2 in. cold-rolled steel shielding, drive the rotation with a stainless steel drive shaft and turn a potentiometer used for position readout. Compressed air is used for insertion and retraction. The slits are water cooled, and have interchangeable tips. Closing a ball valve after partially removing the phase slit shaft, protects the vacuum while removing the shaft to change pin sizes.

2.2. Phase Selection Calculations

Central ray orbits for 40 Mev/A $^4He^{1+}$ were obtained with the program CYCLONE[5] for RF starting times of $\tau_0 = 210° - 236°$ every 2°, where $\tau_0 = 270°$ is the peak voltage on the dee. The magnetic field and central region electric field were obtained with MONSTER[6] and RELAX3D[7] respectively. A first harmonic magnetic bump was used in CYCLONE to center $\tau_0 = 220°$ at 80 turns. SOMA[3,8] was then run to accelerate uniformly populated eigen-ellipses in (r, p_r) phase space of area 100π mm-mrad about each central ray. The slit's diameter and radius were selected to pass $\tau_0 = 220°$, cutting all other times that make it through the central region. All rays that intercepted the slits were removed. The resulting transmission for two slits is a nearly triangular shape with a FWHM of 7° in τ_0 (see Fig. 5.) Three slits gave a FWHM of 5°.
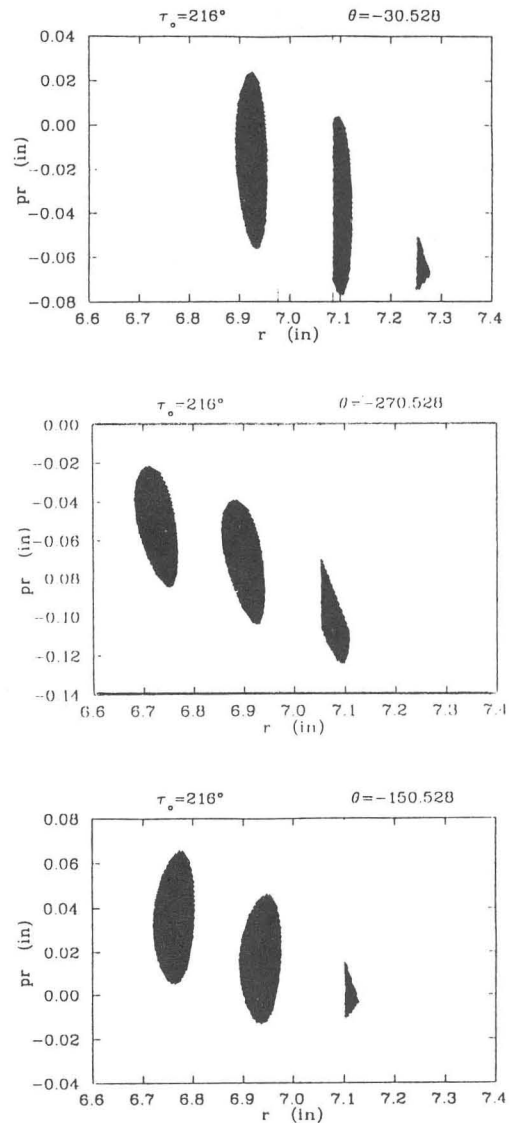

Figure 4. Snap shots, calculated with SOMA, of the (r, p_r) phase space, showing the cuts made by the pins on turns 17 and 18, for $\tau_0 = 216°$. The pins transmit all of $\tau_0 = 220°$. Note the $\sim 120°$ rotation in the (r, p_r) plane as the beam traverses 120° in the machine. At this radius $\tau_0 = 216°$ trails $\tau_0 = 220°$ in energy gain, so the innermost edge is cut by the pin. Starting times that lead $\tau_0 = 220°$ in energy gain have the outermost edge cut. Here, differences in centering errors are small enough to be a perturbation in the $r - \phi$ correlation of the phases of interest.
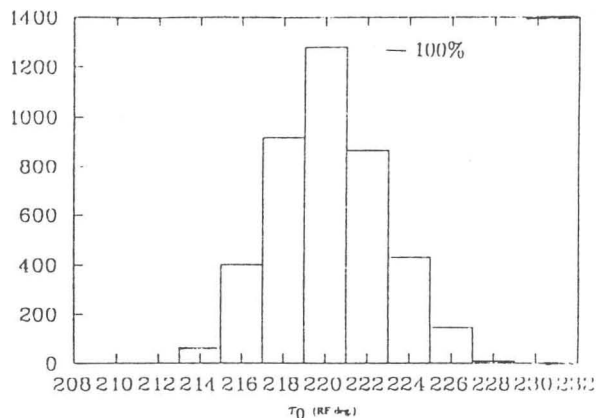
Figure 5. Calculated transmission through the phase slits, for two slits spaced 120° apart. The scale in x is starting time in RF degrees of each eigen-ellipse. Up to this point, there has been RF phase focussing, reducing the RF phase spread by 25%.
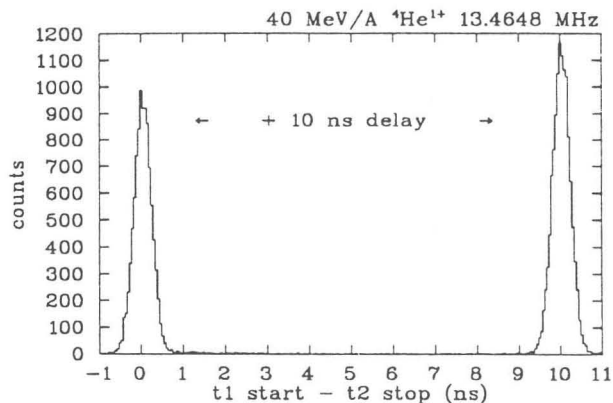

Figure 6. Time resolution of two Si PIN diodes. The second peak was obtained with an extra 10 ns delay to calibrate the TDC. FWHM is .48 ns, giving a resolution of .34 ns in each detector.

3. EXTERNAL PHASE MEASUREMENTS

Attenuators in use in the injection line of the K1200[9] can reduce the beam down to a factor of 3×10^{-7}. This reduction is such that a Si detector, placed to intercept the entire beam, can be used to measure the time of incidence of each beam particle relative to a stop signal generated by the RF. These signals are digitized, then stored in our VAX system, where they can be displayed and saved, via a CAMAC interface. Thus a short integration of counts can give a rapid measurement of the beam's relative distribution in time.

3.1. Measuring Apparatus

The detectors are two 300μ thick $18 \times 18mm^2$ Si PIN diodes mounted back to back in a beam diagnostic chamber 10 ft. from the cyclotron. They are mounted on a two position drive, with the first position scintillating plate mounted 45° to the vertical. A CCD camera focused on the scintillator gives the feedback necessary to tune the beam envelope onto the detector, using the first three beamline quadrupoles.

An LBL Time Pickoff obtains a fast time signal by inductively coupling a pre-amp to the transmission line between an over depleted diode and its charge sensitive pre-amp. Fast signals from each diode are amplified then input into a constant fraction discriminator. The forward diode's CFD output is used to start the time to digital converter. The TDC stops are from a zero crossing discriminator reading an inductive loop in one of the dee stems, and from the TDC of the second detector.

The detector to detector time resolution measured with a 40 MeV/A ^{4}He incident beam is shown in Fig. 6. The wide range of beam energies and atomic charges that the K1200 is capable of providing[10] result in a wide variation in signal strength (< 1 MeV to several GeV.) The above beam deposits $\simeq$ 1 MeV in each detector. This close to the cyclotron, the RF noise is a significant

problem, and ions with greater signal strength are easier to detect. In the stability measurements, one narrow peak was measured at .34 ns FWHM.

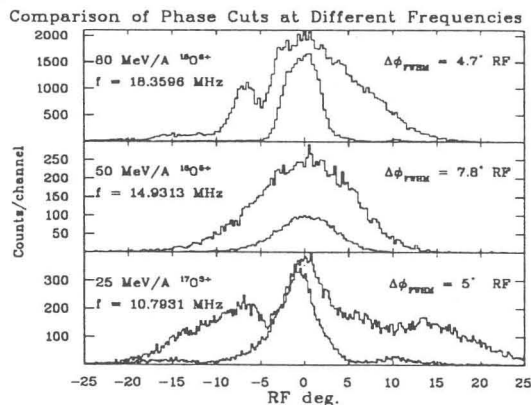### 3.2. Phase Selection Measurements

Figure 7. A comparison of extracted beam time structure at different frequencies. Each graph has been scaled so that the ratio of areas under the curves corresponds to the ratio of the measured intensities. The cuts made by the phase slits appear to be independent of frequency.

The phase slits have been fully operational since Jan. '92. In tuning the slits, it is easiest to individually scan each slit through the beam, noting the minima and maxima in transmitted intensity associated with turn structure. Then starting with the slits in convenient minima, adjust them to select some favorable portion of the uncut distribution. This procedure helps in maximizing transmission through the slits.

Table 1. shows that cuts from 4° to 8° FWHM have been consistently achieved, with transmission of $\sim$ 25 $-$ 30% of the uncut beam. Figure 7. shows that the cuts seem to be independent of operating frequency. This is possible, because the operating parameters for

Table 1. Phase cuts and transmission.

Ion	Energy (MeV/A)	ϕ_{FWHM} uncut	ϕ_{FWHM} cut	I_{cut}/I_0
$^{17}O^{3+}$	25	15.°RF	5.7°RF	.33
$^{16}O^{5+}$	50	12.7°RF	7.8°RF	.24
			6.6°RF	—
$^{24}Mg^{7+10)}$	60	11.°RF	2.6°RF	.25
$^{18}O^{6+}$	80	14.5°RF	4.7°RF	.30
$^{28}Si^{9+}$	80	12.°RF	4.6°RF	.23
			3.6°RF	—

each beam are set to give the same path through the fixed central region.
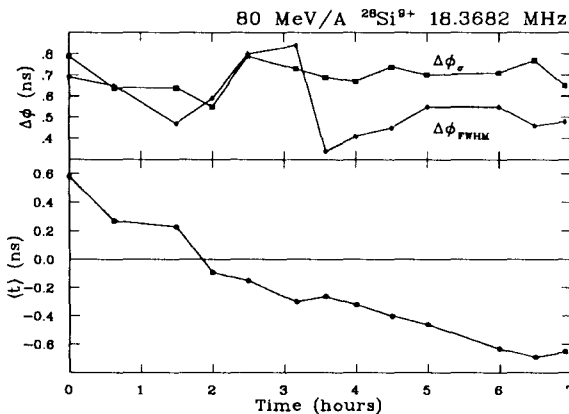
3.3. Phase Stability Measurement

Figure 8. Tracking, over time, of the extracted beam time structure transmitted through the phase slits. Presented are the first and second moments, and the FWHM of the main peak. The cyclotron was not retuned during this time. The centroid drifted, and the structure fluctuated.

The stability of the phase reductions in the extracted beam was monitored over a seven hour period. During this time, the operators did not readjust the cyclotron settings. Figure 8. shows the time centroid of the beam drifting with respect to the RF stop signal at an almost constant rate. It was found that the uncut beam had shifted the same amount during this measurement. The source of this shift is not known, but it is a change of 2 parts in 10^5 of the ~ 800 turns inside the machine. The need to periodically retune the cyclotron, and the variation in time structure shown in Fig. 8., together with this drift show a need for continual monitoring of this time structure.

4. INTERNAL PHASE PROBE

An internal timing probe for the K1200 is being made. It will be interchangeable with the radial current and scintillator probes now in use.[11] A significant

problem is the tight turn spacing in the outer radius of the machine. To extend the active area of the detector to it's edge, detectors have been developed that are cut along the inner guard ring.[12]

This probe will enable us to separate the effects of extraction from those of the probe. It will be used to study beam dynamics during extraction, and measure the outer part of the phase curve inside the machine. There are also plans to use it in tuning the cyclotron at extreme lows in intensity.

5. REFERENCES

1) Nolen, J., et al., "Commissioning Experience with the NSCL K1200 Superconducting Cyclotron," in **Proc. of the 12th Int. Conf. on Cyclotrons and Their Applications** (World Scientific, Singapore, 1991) p.6.
2) Marti, F., and Gavalya, A., "Axial Injection in the K500 Superconducting Cyclotron," in **Proc. of the 11th Int. Conf. on Cyclotrons and Their Applications** (Ionics, Tokyo, 1987) pp.484–487.
3) Milton, B., "Phase Selection in the K500 Cyclotron and the Development of a Non-Linear Transfer Matrix Program," Ph. D. Thesis, Michigan State University, 1986.
4) Milton, B., et al., "Design of a Beam Phase Measurement and Selection System for the M.S.U. K500 Cyclotron," in **Proc. of the 10th Int. Conf. on Cyclotrons and Their Applications** (IEEE, New York, 1984) pp.55–58.
5) Marti, F., et al., "Design Calculation for the Central Region of the NSCL 500 MeV Superconducting Cyclotron," in **Proc. of the 9th Int. Conf. on Cyclotrons and Their Applications** (les Éditions de Physique, Caen, 1981) pp.465–468.
6) Harwood, L., "Status of Integrated Software Project for Cyclotron Design," MSU National Superconducting Cyclotron Laboratory Annual Report (1986) pp.147–148.
7) Houtman, H., and Kost, C., "Design Calculation for the Central Region of the NSCL 500 MeV Superconducting Cyclotron," in **Proc. of the Europhysics Conference on Computing in Accelerator Design and Operation** (Springer-Verlag, Berlin, 1983) pp.98–103.
8) Milton, B., "A Cyclotron Orbit Code Using Second Order Transfer Matrices," in **Proc. of the 11th Int. Conf. on Cyclotrons and Their Applications** (Ionics, Tokyo, 1987) pp.240–243.
9) Cole, D., et al., "ECR Operation Summary," MSU National Superconducting Cyclotron Laboratory Annual Report (1990) pp.147–148.
10) Miller, P., et al., "Performance of the K1200 Cyclotron at MSU," these Proceedings.
11) Marti, F., "Internal Beam Dynamics with a TV Probe," these Proceedings.
12) Evensen, L., Private communication, Senter for Industriforskning, Norway, 1992.